An Ergonomic Shared Workspace Analysis Framework for the Optimal Placement of a Compact Master Control Console

Dandan Zhang, *Student Member, IEEE*, Jindong Liu, *Senior Member, IEEE*, Anzhu Gao, *Member, IEEE*, and Guang-Zhong Yang, *Fellow, IEEE*

***Abstract*—Master-Slave control is commonly used for Robot-Assisted Minimally Invasive Surgery (RAMIS). The configuration, as well as the placement of the master manipulators, can influence the remote control performance. An ergonomic shared workspace analysis framework is proposed in this letter. Combined with the workspace of the master manipulators and the human arms, the human-robot interaction workspace can be generated. The optimal master robot placement can be determined based on three criteria: 1) interaction workspace volume, 2) interaction workspace quality, and 3) intuitiveness for slave robot control. Experimental verification of the platform is conducted on a da Vinci Research Kit (dVRK). An in-house compact master manipulator (Hamlyn CRM) is used as the master robot and the da Vinci robot is used as the slave robot. Comparisons are made between with and without using design optimization to validate the effectiveness of the ergonomic shared workspace analysis technique. Results indicate that the proposed ergonomic shared workspace analysis can improve the performance of teleoperation in terms of task completion time and the number of clutching required during operation.**

***Index Terms*—Learning and adaptive systems, telerobotics and teleoperation, medical robots and systems.**

I. Introduction

RECENT years have seen the increasing use of robot-assisted surgery for minimally invasive surgery [1]. To this end, the master-slave paradigm is used extensively for human-robot interaction, where a master controller is employed to seamlessly relay a surgeon's manoeuvre to the slave robot. To ensure ease of routine clinical use, compact master manipulators are attractive for surgical training and clinical deployment, since they have inherent advantages such as small footprint and are easy-to-setup properties [2], [3].

A master control console is an interface where robots collaborate with humans in a shared environment. To assist the operator to perform a precise manipulation task, analysis of the Human-Robot workspace for Interaction (HRI) can provide ergonomic support to help human reduce fatigue. Therefore, ergonomics is an important aspect of design consideration [4], which can influence the desired manipulation performance. With appropriate ergonomic design, the operator can feel more comfortable and confident to conduct surgical tasks with higher efficiency. Therefore, the configuration and placement of the master manipulator should be optimized to facilitate ergonomic manipulation of the surgical robots [5].

For ergonomic consideration among HRI applications, optimal humanoid robot design has been investigated to support robot for online queries such as grasping or solving inverse kinematics [6], [7]. Except for the workspace modeling of the robot, human operator modeling is significant for HRI consideration. For example, a probabilistic representation of human workspace was proposed in [8], which analyzed the human motion range and reachable workspace, while a Master Motor Map (MMM) framework has been proposed for human arm workspace modelling and analysis in [9]. However, the studies mentioned above are not targeted for surgical remote control application. The model can be more specific based on the characteristics of the master-slave operational mode.

As for surgical applications, maintaining a good body posture for the surgeon during robot-assisted surgery has been analyzed for the da Vinci console [10]. However, its main focus was on geometric data and ergonomic instructions for an optimal console setting without considering the master manipulators. The placement of the da Vinci Surgical System has been explored to maximize the performance of the robot in the surgical site [11], but the placement of master robots has not been explored yet.

In order to realize safe and precise operation for surgical robot remote control, hand motions of an operator are analyzed in [12], [13], with the main focus on task characteristics for neural surgery to optimize the kinematics. However, it didn't consider the mutual effects brought by the human operator, master and slave robots, leading to a general model.

The intuitiveness of master-slave control should be ensured to further enhance the control efficiency during surgical teleoperation. Even if the slave robot has sufficient dexterity to perform a complicated task with high precision, surgeons will not be satisfied with the usability of the master controller if the similarity of the gripping pose between the master and slave

Manuscript received September 6, 2019; accepted January 23, 2020. Date of publication February 17, 2020; date of current version March 2, 2020. This letter was recommended for publication by Associate Editor M. Zecca and Editor P. Valdastri upon evaluation of the reviewers' comments. *(Corresponding authors: Dandan Zhang; Guang-Zhong Yang.)*

Dandan Zhang and Jindong Liu are with the Hamlyn Centre for Robotic Surgery, Imperial College London, London SW7 2AZ, U.K. (e-mail: d.zhang17@imperial.ac.uk; jindong.liu@gmail.com).

Anzhu Gao and Guang-Zhong Yang are with the Hamlyn Centre for Robotic Surgery, Imperial College London, London SW7 2AZ, U.K., and also with the Institute of Medical Robotics, Shanghai Jiao Tong University, Shanghai 200240, China (e-mail: gaoanzhu@hotmail.com; gzyang@sjtu.edu.cn).

Digital Object Identifier 10.1109/LRA.2020.2974428

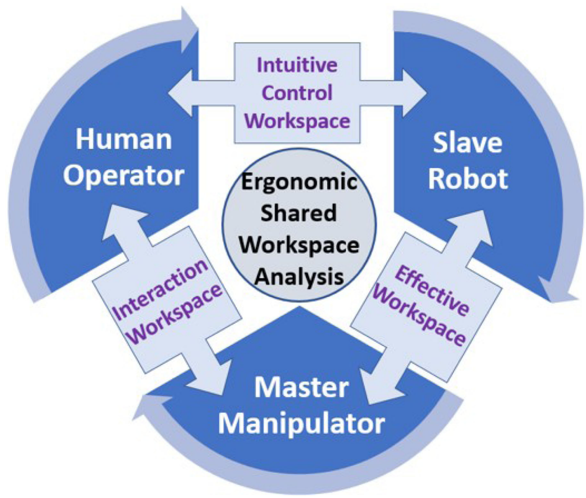

Fig. 1. An overview of the ergonomic shared workspace analysis framework.

robot can not be ensured [5]. The slave robot cannot reach its full potential if paired with an unsuitable master manipulator.

Thus far, the design theory of the slave system has been studied actively, while the optimal design of master control has not been fully explored [14]. In practice, a design process should take the intrinsic and extrinsic indices into consideration. Intrinsic indices are unrelated to the manipulators' task or application [15], while extrinsic indices are task-specific. We endeavor to focus on the extrinsic indices in this letter with the main emphasis on ergonomic operation for RAMIS in this letter, while the description of the configuration selection and performance evaluation have been presented in [16]. The ultimate goal and the main contribution of this letter are to develop a theory for optimal placement of a compact master control console which can enable the operators to conduct surgical tasks with high efficiency.

The remainder of this letter is illustrated as follows. Section II illustrates the design theory, i.e., the ergonomic shared workspace analysis framework. Section III introduces the process for optimal design with a detailed case study. User studies based on a ring transfer task are illustrated in Section IV with results analysis and discussions. Conclusions are drawn in Section V.

II. Methodology

In this section, the design concept and the overview of the ergonomic shared workspace analysis framework are illustrated. Several key components for workspace analysis are analyzed subsequently.

A. Overview

Fig. 1 indicates the relationship among human operator, master manipulator and slave robot, which illustrates the overall theoretical design considerations for this letter. The workspace of the slave robot, the master robot and the human operator are analyzed first. The effective workspace has been proposed in [16] for master manipulator configuration selection while taking the targeted operational scenes into consideration. Moreover, in pursuit of high-efficiency teleoperation performance, the workspace of slave robots when conducting surgical tasks and the human operator workspace should be analyzed jointly to incorporate intuitive control requirements into the framework. To ensure ergonomics, the shared workspace where interaction is conducted between the human operator and the master manipulator should be optimized. Several key workspace analysis and the interaction workspace generation are illustrated as follows.

B. Bimanual Workspace Generation

Workspace generation is to form a point cloud of the reachable positions in the Cartesian space when the robotic manipulator runs through all possible configurations in the joint space [17]. In order to realize numerical calculation, discretized workspace representation in volume data mode is necessary.

For workspace quality evaluation, $\mathcal{W}_m$ is denoted as the local indices distribution map. $\mathcal{W}_m = \{[\boldsymbol{p}(\mathbf{x},\mathbf{y},\mathbf{z}), \mathbf{s_m}(\boldsymbol{p})] = [\mathbf{f}(\mathbf{q}), \mathbf{I_m}(\mathbf{q})] \mid \mathbf{q_{min}} \le \mathbf{q} \le \mathbf{q}_{\max}\}$, where $\boldsymbol{p}(\mathbf{x},\mathbf{y},\mathbf{z}) \in \mathbb{R}^3$ is the 3D end-effector position in a Cartesian space. $\mathbf{q} \in \mathbb{R}^n$, $\mathbf{q_{min}}$ and $\mathbf{q}_{\max}$ represent the lower and upper joint limits respectively. $\mathbf{f}(\cdot)$ is the forward kinematics of the robot, which is described by $\mathbb{R}^n \to \mathbb{R}^3$. $\boldsymbol{I_m}(\mathbf{q})$ indicates the m_{th} local evaluation index value for a given robot when the robot has a configuration of $\mathbf{q}$, while $\mathbf{s_m}(\mathbf{p})$ represents the local evaluation index value for a given robot when the 3D end-effector position is at $\boldsymbol{p}$. The voxel value can represent the local indices evaluation information, which describes the capabilities of the robot. $V_m \in R_V$ is the volume data transformed by $\mathcal{W}_m$, where R_V is a space with voxel data, the dimension of which is 4D.More detailed explanation of the local distribution map and volume data generation can be found in [18].

Generally, the surgical robot is controlled through bimanual operations, generating the workspace for a single robot is not enough. Therefore, a bimanual robot workspace combination operation is defined as $V_{Lm} \uplus V_{Rm}$. This operation is used for two robots with the same configuration. The range of the workspace of the left and right manipulator is registered before the calculation, which means that the volume data has the same size and boundary. The operation result $V_{Bm} = V_{Lm} \uplus V_{Rm}$ is defined as follows.

$$V_{Bm} = \sum_{i=1}^{i\max} \sum_{j=1}^{j\max} \sum_{k=1}^{k\max} [(V_{Lm}(i,j,k) + V_{Rm}(i,j,k))] \quad (1)$$

All the workspace analyse are based on bimanual robots in this letter. The workflow and details of the construction of the ergonomic shared workspace are described as follows.

C. Master Manipulator Dexterous Workspace

The dexterous workspace of the master manipulator can be generated based on three common evaluation indices, i.e. i) manipulability, ii) inverse condition number and iii) minimal singular value, which analyzes the workspace quality across the whole reachable workspace.

$J(\boldsymbol{q})$ is the Jacobian matrix of the manipulator. By using the singular value decomposition, the Jacobian matrix can be decomposed to $\sigma_i(i = 1, 2 \ldots m)$. The definitions of the three evaluation indices are shown as follows.

1) Manipulability: Manipulability ($\boldsymbol{I_1(q)}$) represents the distance from a given pose of the manipulator to a singular configuration [19], which is defined as $I_1(\boldsymbol{q}) = \sqrt{det(J(\boldsymbol{q})J(\boldsymbol{q})^T)}$.

2) Inversed Condition Number: Inversed condition number ($\boldsymbol{I_2(q)}$) represents the distance to the kinematic isotropy of the Jacobian [20], which is defined as $1/||J(\boldsymbol{q})||{\cdot}||J(\boldsymbol{q})^{-1}||$.

3) Minimum Singular Value: Minimum singular value ($\boldsymbol{I_3(q)}$) represents an upper bound for the velocity with which the manipulator can move in all directions [20], which is defined as $I_3(\boldsymbol{q}) = \min(\sigma_1, \sigma_2, \ldots, \sigma_m)$.

For an overall evaluation, the global modified index G is defined as the integral of the normalized local index over the whole reachable workspace. The larger the G value, the better the quality of the workspace of the robot, and thus the higher average workspace quality can be achieved. More detailed explanation of the modified global indices calculation can be found in [18].

D. Human Operator Comfortable Workspace

Modeling the comfortable workspace of the human arm is essential for ergonomics consideration. In [5], human comfortable operation space is defined, it was said that human may have comfortable operation space in sector-shaped with height 300 mm, radius 200 mm and angle 45° when the slave manipulator's working space is an inverted cone with height 250 mm and taper angle 60°. However, this comfortable operation space analysis is not for the surgical remote control application purpose. A more reasonable human operation model for RAMIS should be built up.

Human arms have 7 Degree-of-freedom (DoFs), 3 DoFs for shoulder, one DoF for elbow, and the remaining 3 DoFs at the wrist. Though human motion is represented in [21], it is not necessary to build up the whole reachable workspace of human arms, because the motions of surgical operation are constrained in the control console.

To control the master manipulators, operators normally rest their arms on the armrest and hold the end-effectors of the manipulators using the thumb and fingers. General motions include forward/backward, lateral movements, pitch and roll motions on the fulcrum of the armrest, and 3D wrist motions. The analysis of the operation motions of surgeons and the corresponding equivalent model of human operator for surgical teleoperation are shown in Fig. 2. The linear motions of moving the arms left and right, forward and backward are generated by the movements of the shoulder, which can be regarded as two prismatic joints for changing the resting point of the operators' arms. The pitch and yaw motions of the elbow can be known as a universal joint with 2 DoFs while the wrist motions of the operator can be considered as a spherical joint with 3 DoFs.

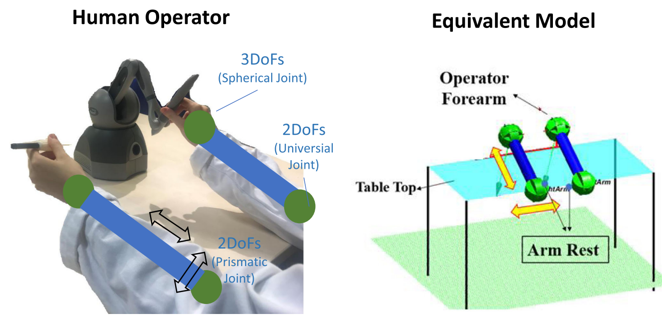

Fig. 2. The analysis of operation motion of surgeons and the corresponding equivalent model of human operator for surgical teleoperation.

TABLE I
DH TABLE AND JOINT LIMITS FOR THE HUMAN OPERATOR EQUIVALENT MODEL

	1	2	3	4	5	6	7
α	90	90	-90	0	0	0	0
a_i	0	0	0	0	0	90	90
d_i	d_1	0	0	d_2	0	0	0
θ_i	0	θ_2	θ_3	0	θ_5	θ_6	θ_7
θ_{di}	0	70	170	θ_{d4}	140	160	90
θ_{ui}	0.20	-70	10	θ_{u4}	-140	20	-90

Note: The unit for the angle of the revolute joint is degree.
The unit for the link offset/prismatic joint limit is metre.

Based on the general movements mentioned above, the human operator comfortable workspace can be built up for ergonomics consideration.

For workspace generation, an equivalent Denavit–Hartenberg (DH) table is defined in Table I. θ_{ui} and θ_{di} represent the upper and lower boundary for the joint limit of the equivalent model respectively. θ_{u4} and θ_{d4} can be slightly adjusted based on the arm-length and operational habits of different operators.

E. Slave Robot Operational Workspace Analysis

There are various types of slave robots. The purpose for the slave robot operational workspace analysis is to ensure that the configuration of the master robot is suitable, while the placement of the master manipulator can provide the operator with the sense of intuitive control to fulfill a surgical task.

After being inserted to the operational targets, surgical instruments have a desirable working range around the trocar during the RAMIS. Due to the fulcrum effect, the trocar limits the motion of manipulators to two rotational movements at the fulcrum point, one translational movement insertion displacement along the longitudinal axis, one rotational movement of the tool [22]. Therefore, the slave robot operational workspace can be generated.

The main target for the slave robot operational workspace analysis is to generate the dexterous workspace and find out the characteristic angle which has the maximum probability of reaching the highest dexterity for orientation control. Different types of surgeries may have different characteristic angles.

As for MIS, the most dexterous direction is normally coincided with the central line of the trocar.

F. Intuitive Control Workspace

Intuitive control is important to seamlessly relay the surgeons' intention to the surgical robot, which means that the orientation of the master manipulator's end-effector has the same direction as the slave robot's end-effector. This can ensure the dexterous orientation control during teleoperation. To ensure the ergonomic effects for a human operator, it is desirable when the human operators can control the master manipulator without bending their wrists at large angles. In this way, the operators have maximum flexibility and can realize remote control in the most natural way.

The maximum dexterous distribution of human wrist $\boldsymbol{H(q_h)}$ can be calculated, where $\mathbf{q_h} \in \mathbb{R}^n$ is the human operator equivalent model joint vector. It represents the direction where human has maximum flexibility for orientation control. The evaluation metric of intuitiveness for the left and right hands of the operator is defined as $I_4(\boldsymbol{q_h})$ (see (2)), when the joint vector for the equivalent model is $\boldsymbol{q_h}$.

$$I_4(\boldsymbol{q_h}) = 1 - \frac{\boldsymbol{p_*}\cdot \boldsymbol{H(q_h)}}{||\boldsymbol{p_*}||\cdot||\boldsymbol{H(q_h)}||}(* = l, r) \tag{2}$$

$\boldsymbol{p}_l$ and $\boldsymbol{p}_r$ are the vectors that represent the most dexterous direction for the left and right surgical tool during the MIS operation respectively, which can be tuned based on different applications. The intuitive control workspace can be calculated for the left and right arms respectively and then combined via (1). The smaller the angle between the operator dexterous control motion and the slave robot dexterous central line is, the higher the value of $I_4(\boldsymbol{q_h})$ is, the more intuitive control can be realized at this pose.

G. Interaction Workspace

The shared workspace generation can be obtained for further analysis after considering the workspace analysis results of the master manipulator and the human operator. The workspace combination and intersection of two heterogeneous robots are defined as $V_{Am} \bigcup V_{Bm}$ and $V_{Am} \bigcap V_{Bm}$, the results of which are V_B and V_I respectively.

$$V_B = \sum_{i=1}^{i\max}\sum_{j=1}^{j\max}\sum_{k=1}^{k\max} [(V_{Am}(i,j,k) \wedge V_{Bm}(i,j,k))] \tag{3}$$

$$V_I = \sum_{i=1}^{i\max}\sum_{j=1}^{j\max}\sum_{k=1}^{k\max} [(V_{Am}(i,j,k) \vee V_{Bm}(i,j,k))] \tag{4}$$

In this way, the volume and boundary of the overall reachable workspace and the intersection workspace volume can be easily obtained, which paves a way for further shared workspace quality evaluation.

III. Optimal Design

In this section, an Ergonomic Shared Workspace Index ($ESWI$) is proposed. A case study will be provided to illustrate the overall process of optimal design for ergonomic considerations.

A. Ergonomic Shared Workspace Analysis

In this study, $V_E = V_{Am} \sqcup V_{Bm}$ is used to represent the workspace combination of two heterogeneous robots, while $V_C = V_{Am} \sqcap V_{Bm}$ is used to represent the workspace quality evaluation of one robot within the reachable workspace of another robot.

$$V_E = \sum_{i=1}^{i\max}\sum_{j=1}^{j\max}\sum_{k=1}^{k\max} [(V_{Am}(i,j,k) \times V_{Bm}(i,j,k))] \tag{5}$$

$$V_C = (V_{Am} \sqcup \mathcal{V}_{Bm}) \sqcup \left(V_{Am} \bigcap V_{Bm}\right) \tag{6}$$

Base on the DH table of the targeted master manipulator for optimization, the reachable workspace and the three workspace with local index distribution of the master manipulator can be represented as V_{B0}, V_{B1}, V_{B2} and V_{B3} respectively. The human operator comfortable workspace is denoted as V_{H0}, while the intuitive control workspace is denoted as S_H.

In order to make good use of the master manipulator, the master manipulator's workspace should have the maximize intersection with the human arms' comfortable moving space, while the workspace quality of the intersection area should be optimized. Therefore, several objective functions can be defined as follows.

$$\begin{cases} F_1 = \mathcal{B}(\mathcal{V}_{H0} \bigcap \mathcal{V}_{B0}) \\ F_2^i = G(\mathcal{V}_{H0} \sqcap \mathcal{V}_{Bi})(i = 1,2,3) \\ F_3 = G(\mathcal{S}_H \sqcap \mathcal{V}_{B0}) \end{cases} \tag{7}$$

where $\mathcal{B}(.)$ is the operator for the targeted workspace volume acquisition, $G(.)$ is the operator of global workspace quality evaluation. F_1 represents the volume of the shared workspace generated by the human operator comfortable workspace and the master manipulator reachable workspace. $\mathcal{V}_{H0} \sqcap \mathcal{V}_{Bi}(i = 1,2,3)$ represent the local indices distribution of the master manipulator within the shared workspace, while $F_2^i(i = 1,2,3)$ reflects the global performance of the master manipulator within the shared workspace. F_3 indicates the intuitiveness for control in the shared workspace.

B. Ergonomic Shared Workspace Index

In order to take all the objective functions in (7) into consideration, AHP is used [23], which leads to the definition of the Ergonomic Shared Workspace Index ($ESWI$).

A preference matrix $A = [a_{ij}](a_{ji} = 1/a_{ij})$ for decision-making is generated to calculate the weights of the objective functions, the element of which is based on pairwise comparisons by comparing elements i and j. Normally, the judgment scale ranges from 1 to 9, where 9 indicates absolutely importance. Suppose that the dimension of the preference matrix is $n \times n$, w_i can be obtained as the weight for each element after normalization. The diagram of the $ESWI$ generation is shown in Fig. 3.

To check the consistency of the preference matrix, a random consistency index table is utilized to verify the consistency

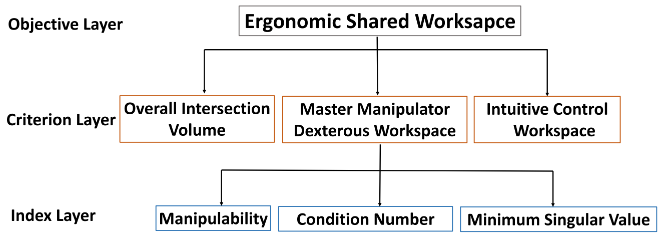

Fig. 3. Schematic diagram of the construction of the AHP based ergonomics hared workspace analysis framework.

ratio $CR = \frac{\lambda_{\max}-n}{r(n-1)}$ [24], [25], where $\lambda_{\max} = \frac{1}{n}\sum_{i=1}^{n}\frac{(Aw)_i}{w_i}$. $r = 0.58$ is used in this letter, since $n = 3$ [24]. The consistency can be verified if the value of CR is smaller than 0.1. w_p^c and w_{pq}^i is the weight for the p_{th} index in the criteria layer and the weight for the q_{th} index in the index layer under the p_{th} criteria layer respectively. I_{pq} indicates the evaluation value for the q_{th} index of the p_{th} criteria. The $ESWI$ is defined as follows:

$$ESWI = \sum_{p=1}^{n_c}\sum_{q=1}^{n_p} w_p^c w_{pq}^i \cdot I_{pq} \tag{8}$$

where $n_c = 3$ is the number of metrics in the criteria layer, n_p is the number of metrics in the index layer under the p_{th} metric of the criteria layer. In this case, n_p is equal to 1 for the first and third criteria layer, while n_p is equal to 3 for the second criteria layer.

For practical considerations, the placement of the robot should not be too closed to the human operator, which constrains the operators' movement. It cannot be too far away from the human, which may reduce the interaction volume significantly. To reduce the parameter during the optimal design process, assumptions are required. In this letter, we assumed that the central line between the bimanual master manipulators coincides with the central lines of the human operator. Therefore, the transition value in the x-axis is equal to zeros.

The coordinate of the human operator equivalent model ($O - XYZ$) and that of the master manipulators ($O_m - X_mY_mZ_m$) are shown in Fig. 4, where $O - XYZ$ can be regarded as the global coordinate. The initial translation vector between O_m and O is $P_o = [0, Y_o, Z_o]m$, where $Y_o = 0.40\ m$ and $Z_o = -0.40\ m$.

In the above Y and Z are two variables for optimization, which represents the translation distance in the direction of y-axis and z-axis compared to the initial placement before optimization. The variable Y and Z for optimization and the range for consideration is $[-0.1\ m, 0.2\ m]$ and $[-0.15\ m, 0.15\ m]$ respectively. Considering that the placement does not need to be very accurate, the variables for optimization are sampled in discrete form, with an interval of 0.01 m. The errors of numerical calculation for workspace analysis are acceptable.

To summarize the ergonomic workspace analysis framework, an algorithm description is provided as shown in Algorithm **1**. Suppose that the targeted master manipulator for analysis is predesigned, the parameters of human operator equivalent model can be confirmed. A list of potential configuration and robot

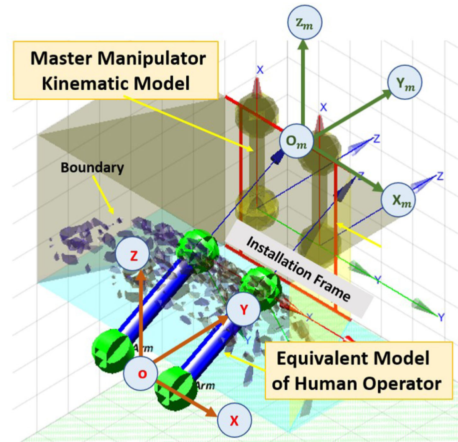

Fig. 4. Coordinate of the human operator equivalent model and the master manipulators.

Algorithm 1: Ergonomic Workspace Analysis Framework.

Input: $\boldsymbol{P(i)} (i = 1, 2 \ldots K)$
1: Calculate Initial $\mathcal{V}_{B0}(\boldsymbol{P_o})$ based on (1)(3).
2: Calculate Initial $\mathcal{V}_{B1}(\boldsymbol{P_o})$, $\mathcal{V}_{B2}(\boldsymbol{P_o})$ and $\mathcal{V}_{B3}(\boldsymbol{P_o})$ based on (1)(4)(6).
3: Calculate $\mathcal{V}_H$ and $\mathcal{S}_H$ based on (1)(2)(6).
4: **for** $i = 1 : 1 : K$ **do**
5: Obtain $\mathcal{V}_{B0}(\boldsymbol{P(i)})$, $\mathcal{V}_{B1}(\boldsymbol{P(i)})$, $\mathcal{V}_{B2}(\boldsymbol{P(i)})$ and $\mathcal{V}_{B3}(\boldsymbol{P(i)})$
6: Calculate F_1, $F_{2i} (i = 1, 2, 3)$, F_3 based on (7)
7: Calculate $\boldsymbol{E(P(i))}$ based on (8)
8: **end for**
9: Find out $\boldsymbol{E}_{\max}$ among $\boldsymbol{E(P(i))} (i = 1, 2, \ldots K)$, Y_m, Z_m.
Output: $\boldsymbol{P_f}$.

placement $\boldsymbol{P(i)} (i = 1, 2 \ldots K)$ is used as the input for optimal design. $\boldsymbol{P(i)}$ is the translation vector, which are consist of different combinations of Y and Z. $\boldsymbol{E(P(i))}$ indicates the $ESWI$ value when the robot has configuration of $\boldsymbol{P(i)}$. The maximum $ESWI$ value ($\boldsymbol{E}_{\max}$) and the corresponding placement vector $\boldsymbol{P_f} = [0, (Y_o + Y_m), (Z_o + Z_m)]$ can be determined.

C. Case Studies

The ergonomic shared workspace analysis framework is general for different users and surgical applications. A case study is provided here for concept demonstration.

1) Master Manipulator: Hamlyn CRM, a compact master manipulator is used for optimization in this case study, the DH table of which is defined in [16]. Therefore, the master manipulator dexterous workspace can be generated. The CAD model of the Hamlyn CRM is shown in Fig. 5(a), while the operation scenarios is shown in Fig. 5(b).

2) Slave Robot Operational Workspace: For the slave robot operational workspace analysis, an example based on laparoscopic surgery is utilized in this letter. During the laparoscopic

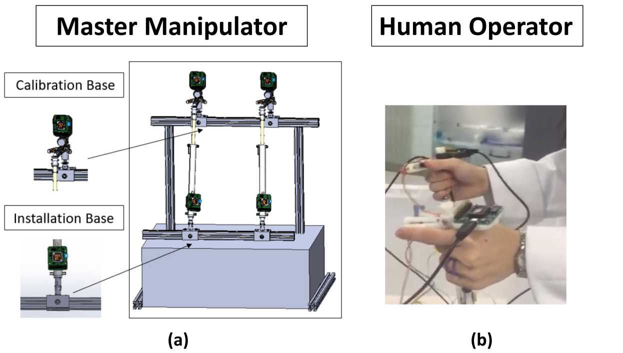

Fig. 5. The master manipulator and the operation scenario. (a) The CAD model of the Hamlyn CRM. (b) The human operator interacted with the master manipulators.

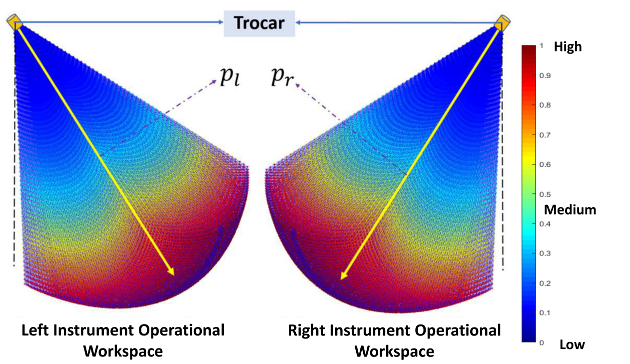

Fig. 6. Dexterity visualization for the surgical instruments.

surgery, two instruments normally form a 60 to 90 degree angle from the tips of instruments for ergonomic operation [26]. Rigid surgical tools inserted through the trocar within the abdominal cavity, are therefore contained by a cone with a vertex angle of sixty degrees during operation [22], [27].

Fig. 6 indicates the workspace analysis results of surgical instruments for minimally invasive laparoscopic surgery. $\boldsymbol{p_l}$ and $\boldsymbol{p_r}$ can be obtained and used as the characteristic angles to represent the direction where the maximum probability of the operation angle is required of the left and right arm of the slave robot during the operation respectively.

3) Human Operator Comfortable Workspace: For the equivalent model of human operator comfortable workspace analysis, $\theta_{d4} = 0.10\ m$ and $\theta_{u4} = 0.30\ m$ are used in this case study. Therefore, the intuitive control workspace can be generated. At each pose, the relative angle between the most dexterous direction of the human arm and the surgical instrument average dexterous direction can be obtained.

4) Construction of the Ergonomic Shared Workspace: Fig. 7 shows the overall process of the ergonomic shared workspace construction. Fig. 7(a) indicates the generation of the reachable workspace boundary and the acquisition of the volume of the shared workspace. The optimal ergonomic shared workspace generated by $\mathcal{V}_{H0} \sqcap \mathcal{V}_{B1}$, $\mathcal{V}_{H0} \sqcap \mathcal{V}_{B2}$, $\mathcal{V}_{H0} \sqcap \mathcal{V}_{B3}$ and $\mathcal{S}_{H} \sqcap \mathcal{V}_{B0}$ can be viewed in Fig. 7(b), (c), (d) and (e) respectively.

AHP method is used to generate different weights for constructing the $ESWI$ for optimization. The preference matrix can be generated by different users. Suppose that C and C_2 for this case study is shown in (9).

$$\boldsymbol{C} = \begin{bmatrix} 1 & 2 & 4 \\ 1/2 & 1 & 2 \\ 1/4 & 1/2 & 1 \end{bmatrix}, \boldsymbol{C2} = \begin{bmatrix} 1 & 2 & 3 \\ 1/2 & 1 & 2 \\ 1/3 & 1/2 & 1 \end{bmatrix} \tag{9}$$

For the criteria layer C and the index layer of C_2, CR can be calculated as 0.008 and 0.048 respectively, both of which are smaller than 0.10. This indicates that the consistency of the preference matrix can be ensured.

The results indicated that the variables of determination of the optimal placement are $Y_m = 0\ m$ and $Z_m = -0.15\ m$ respectively. The final translation vector for the optimal placement of the master robot is $p_f = [0\ m, 0.40\ m, -0.55\ m]$.

IV. User Studies

In this section, detailed illustrations of user studies for validating the proposed framework are presented. Experiments are conducted to test the effectiveness of the proposed theory by comparing the performance of the users when using the master manipulator with and without optimal design.

A. Experimental Protocols

A da Vinci robot is controlled as the slave during user studies. Eight subjects (2 females and 6 males) were invited to join in the user studies based on a ring transfer task. Two users are familiar with dVRK, while three users have prior experience in general teleoperation, and the remaining subjects are novices. All the users practiced the task based on the experimental protocols before the formal user studies.

Illustration of the experimental platform and the ring transfer task is shown in Fig. 8. PSM1 indicates the right surgical instrument while PSM2 indicates the left one. The notations of A, B, C, D, E are shown in Fig. 8. The experimental protocol includes four steps. Firstly, PSM1 is controlled by the user to grasp the ring from A to B. Secondly, PSM2 is controlled by the user to grasp the ring from B to C. Thirdly, PSM1 is expected to grasp the ring from C, pass the ring to PSM2, then place the ring on D. Finally, PSM2 is expected to grasp the ring from D, pass the ring to PSM1, then place the ring on E. The hand motion of the operator measured with a master manipulator is scaled down with a motion-scaling factor of 1/5 using the master-slave control. ∂ is defined as the angle between the z-axis of the world coordinate and the central line of the endoscope. $\partial = 40^\circ$ is set for the user studies.

B. Result Analysis

For objective analysis, standard evaluation metrics can be calculated based on motion data for the quantitative analysis [28]. In this letter, four evaluation metrics are used to evaluate the performance of the subjects during teleoperation, including the total path length of the instruments ST, the task completion time

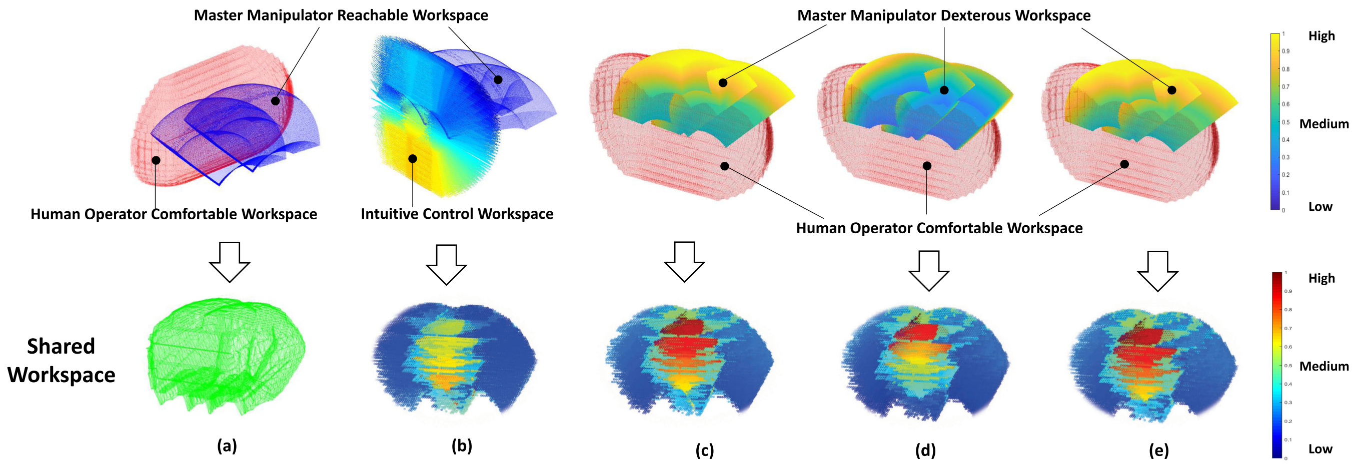

Fig. 7. Visualization of the ergonomic shared workspace construction process. (a) The workspace operation of $\mathcal{V}_{H0} \bigcap \mathcal{V}_{B0}$; The optimal ergonomic shared workspace generated by (b)$\mathcal{V}_{H0} \sqcap \mathcal{V}_{B1}$; (c)$\mathcal{V}_{H0} \sqcap \mathcal{V}_{B2}$; (d)$\mathcal{V}_{H0} \sqcap \mathcal{V}_{B3}$; (e) $\mathcal{S}_{H} \sqcap \mathcal{V}_{B0}$.

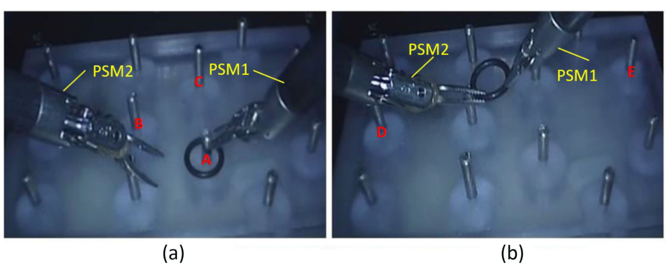

Fig. 8. Illustration of the experimental platform and the ring transfer task.

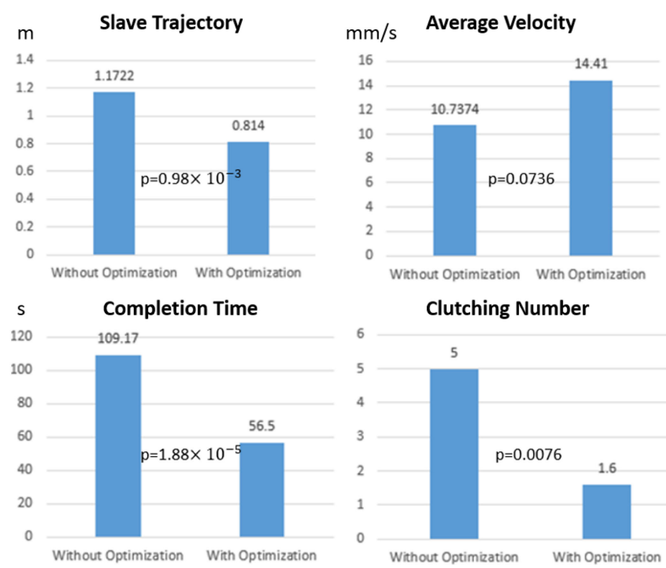

Fig. 9. Results for comparisons between with optimal design and without optimal design, in terms of (a) slave robot trajectory (ST), (b) average velocity (AV), (c) completion time (CT), (d) clutching number (CN).

for a subject to finish the whole procedures of the ring transfer task during one trial CT, the average speed of operation AV, and the number of clutching CN.

The task completion time [29] can identify the fluency of operation for the subjects. It has been reported that when the operators operate in non-ergonomic poses, increased frequency of clutching can be observed due to the improper positioning [30]. Less number of clutching means that the operator is more comfortable with the master controller [31]. As for the path length of the slave robot end-effector trajectory [32], a higher value indicates the reduced straightness of the navigation path for slave robot control [32], which requires more effort from the operator to control the slave robot.

Experimental results show that the master manipulator with optimization can enable the users to have better performance. Fig. 9 shows the results of the comparison. Compared to the trials without optimization, the task completion time for a single trial with optimization is reduced by approximately 50 percent (56.50 s vs. 109.17 s). The clutching number is significantly reduced (1.6 vs. 5). The slave robot end-effector trajectory is reduced (0.814 m vs. 1.172 m), while the average control speed is enhanced (14.41 mm/s vs. 10.74 mm/s).

Normality tests were performed before the analysis of whether the data has statistic differences or not. T-tests were conducted for the metrics which satisfy the normal distribution assumption while Wilcoxon signed-rank tests were conducted for non-parametric statistical comparisons among other variables. The p-values are obtained and are shown in Fig. 9. Except for the average velocity, all the other three evaluation metrics have statistic differences.

C. Discussions

The ergonomic workspace analysis method takes the workspace of the human operator, the slave robot and the master manipulator into consideration. The interaction shared workspace is calculated and analyzed. However, all the calculations are based on numerical calculation. The discrete workspace has inherent errors and the numerical calculation is slow during the iteration process. Therefore, the accuracy of the results needs to be improved. Future work will include exploring the high-efficiency numerical calculation method to obtain more accurate workspace quality evaluation results.

The method proposed in this letter is general, validation on different research platforms can be further explored. Moreover, other types of surgery can be included in the user studies for further verification of the framework's generality for assisting the operator to reach the desired teleoperation performance.

V. Conclusion

In this letter, an ergonomic shared workspace analysis framework is proposed. An optimization method is used to determine the optimal placement of a compact master control console for surgical robot remote control, with the goal of maximizing the usability of the master robot. This plays an important role in improving the outcomes and efficiency of master-slave remote control during robotic surgery.

A prototype, called the Hamlyn CRM, is used for user studies to verify the effectiveness of the proposed ergonomic shared workspace analysis method. Based on the experimental results, it can be concluded that with optimization, the teleoperation efficiency of subjects is significantly enhanced in terms of slave robot end-effector trajectory, average control speed, task completion time and clutching number. Results indicated that using the master manipulator with the ergonomics design, and the operator can feel more comfortable and confident to conduct surgical tasks with higher efficiency.

Acknowledgment

The authors would like to acknowledge all the subjects for taking part in the user studies. The authors would like to acknowledge Dr. Lin Zhang for dVRK facility support and Dr. Yang Hu for valuable discussion.

References

[1] B. Christos and Y. Guang-Zhong, "From passive tool holders to microsurgeodns: safer, smaller, smarter surgical robots," *IEEE Trans. Biomed. Eng.*, vol. 61, no. 5, pp. 1565–1576, May 2014.

[2] V. Vitiello, S.-L. Lee, T. P. Cundy, and G.-Z. Yang, "Emerging robotic platforms for minimally invasive surgery," *IEEE Rev. Biomed. Eng.*, vol. 6, pp. 111–126, Dec. 2012.

[3] C. J. Payne and G.-Z. Yang, "Hand-held medical robots," *Ann. Biomed. Eng.*, vol. 42, no. 8, pp. 1594–1605, 2014.

[4] Z. Thant, S. Low, S. Tang, L. Phee, K. Ho, and S. Chung, "Ergonomic master controller for flexible endoscopic gastrointestinal robot manipulator," in *Proc. Int. Conf. Biomed. Pharmaceutical Eng.*, IEEE, 2006, pp. 575–579.

[5] Y. Kamei *et al.*, "Study on master manipulator design parameters for robotic microsurgery," in *Proc. Biomed. Robot. Biomechatronics 4th IEEE RAS & EMBS Int. Conf.*, 2012, pp. 847–852.

[6] K. Abdel-Malek, W. Yu, and J. Yang, "Placement of robot manipulators to maximize dexterity," *Int. J. Robot. Autom.*, vol. 19, no. 1, pp. 6–14, 2004.

[7] N. Vahrenkamp, T. Asfour, and R. Dillmann, "Robot placement based on reachability inversion," in *Proc. Robot. Autom. IEEE Int. Conf.*, 2013, pp. 1970–1975.

[8] S. C. Venema and B. Hannaford, "A probabilistic representation of human workspace for use in the design of human interface mechanisms," *IEEE/ASME Trans. Mechatronics*, vol. 6, no. 3, pp. 286–294, Sep. 2001.

[9] Ö. Terlemez, S. Ulbrich, C. Mandery, M. Do, N. Vahrenkamp, and T. Asfour, "Master motor map (mmm)—framework and toolkit for capturing, representing, and reproducing human motion on humanoid robots," in *Proc. 14th IEEE-RAS Int. Conf. Humanoid Robot.*, 2014, pp. 894–901.

[10] C. D. Van't Hullenaar, B. Hermans, and I. A. Broeders, "Ergonomic assessment of the da vinci console in robot-assisted surgery," *Innovative Surgical Sci.*, vol. 2, no. 2, pp. 97–104, 2017.

[11] I. Papanikolaidi, A. Synodinos, V. Moulianitis, N. Aspragathos, and E. Xidias, "Optimal base placement of the da vinci system based on the manipulability index," in *Proc. Int. Conf. Intell. Robot. Syst.*, 2013, p. 3.

[12] H. Takahashi *et al.*, "Master manipulator with higher operability designed for micro neuro surgical system," in *Proc. Robot. Autom., IEEE Int. Conf.*, 2008, pp. 3902–3907.

[13] M. Mitsuishi *et al.*, "Master–slave robotic platform and its feasibility study for micro-neurosurgery," *Int. J. Med. Robot. Comput. Assisted Surgery*, vol. 9, no. 2, pp. 180–189, 2013.

[14] M. Bagheri, A. Ajoudani, J. Lee, D. G. Caldwell, and N. G. Tsagarakis, "Kinematic analysis and design considerations for optimal base frame arrangement of humanoid shoulders," in *Proc. IEEE Int. Conf. Robot. Autom.*, 2015, pp. 2710–2715.

[15] G. M. Cloutier, A. Jutard, and M. Bétemps, "A robottask conformance index for the design of robotized cells," *Robot. Auton. Syst.*, vol. 13, no. 4, pp. 233–243, 1994.

[16] D. Zhang, J. Liu, L. Zhang, and G.-Z. Yang, "Design and verification of a portable master manipulator based on an effective workspace analysis framework," in *Proc. IEEE/RSJ Int. Conf. Intell. Robot. Syst.*, Macau, China, 2019, pp. 417–424.

[17] O. Bohigas, M. Manubens, and L. Ros, "A complete method for workspace boundary determination on general structure manipulators," *IEEE Trans. Robot.*, vol. 28, no. 5, pp. 993–1006, Oct. 2012.

[18] D. Zhang, F. Cursi, and G.-Z. Yang, "Wsrender: A workspace analysis and visualization toolbox for robotic manipulator design and verification," *IEEE Robot. Autom. Lett.*, vol. 4, no. 4, pp. 3836–3843, Oct. 2019.

[19] T. Yoshikawa, "Manipulability of robotic mechanisms," *Int. J. Robot. Res.*, vol. 4, no. 2, pp. 3–9, 1985.

[20] J.-O. Kim and K. Khosla, "Dexterity measures for design and control of manipulators," in *Proc. IEEE/RSJ Int. Workshop Intell. Robot. Syst. Intell. Mech. Syst.*, 1991, pp. 758–763.

[21] P. Azad, T. Asfour, and R. Dillmann, "Toward an unified representation for imitation of human motion on humanoids," in *Proc. IEEE Int. Conf. Robot. Autom.*, 2007, pp. 2558–2563.

[22] C. Direkwatana and C. Wilasrusmee, "Workspace analysis for a new design laparoscopic robotic manipulator, "mu-laparobot"," *20th National Grad Research Conf.*, 2011, pp. 2–3.

[23] F. Zahedi, "The analytic hierarchy process—a survey of the method and its applications," *Interfaces*, vol. 16, no. 4, pp. 96–108, 1986.

[24] A.-L. Chicea, R.-E. Breaz, O. Bologa, and S.-G. Racz, "Using serial industrial robots and CAM techniques for manufacturing prosthetic devices," *Appl. Mech. Mater.*, vol. 762, pp. 313–318, 2015.

[25] J. A. Alonso and M. T. Lamata, "Consistency in the analytic hierarchy process: A new approach," *Int. J. Uncertainty, Fuzziness Knowl.-Based Syst.*, vol. 14, no. 04, pp. 445–459, 2006.

[26] U. Matern, P. Waller, C. Giebmeyer, K. D. Rückauer, and E. H. Farthmann, "Ergonomics: Requirements for adjusting the height of laparoscopic operating tables," *J. Soc. Laparoendos. Surg.*, vol. 5, no. 1, p. 7, 2001.

[27] C.-H. Kuo, J. S. Dai, and P. Dasgupta, "Kinematic design considerations for minimally invasive surgical robots: An overview," *Int. J. Med. Robot. Comput. Assisted Surg.*, vol. 8, no. 2, pp. 127–145, 2012.

[28] R. Nagyné Elek and T. Haidegger, "Robot-assisted minimally invasive surgical skill assessment—manual and automated platforms," *Acta Polytech. Hung.*, vol. 16, no. 8, pp. 141–169, 2019.

[29] A. L. Trejos, R. V. Patel, R. A. Malthaner, and C. M. Schlachta, "Development of force-based metrics for skills assessment in minimally invasive surgery," *Surg. Endos.*, vol. 28, no. 7, pp. 2106–2119, 2014.

[30] D. Zhang, B. Xiao, B. Huang, L. Zhang J. Liu, and G.-Z. Yang, "A self-adaptive motion scaling framework for surgical robot remote control," *IEEE Robot. Autom. Lett.*, vol. 4, no. 2, pp. 359–366, 2018.

[31] D. Zhang, J. Chen, W. Li, D. B. Salinas, and G.-Z. Yang, "A microsurgical robot research platform for robot-assisted microsurgery research and training," *Int. J. Comput. Assisted Radiol. Surgery*, vol. 15, no. 1, pp. 15–25, Jan. 1, 2020.

[32] T. N. Judkins, D. Oleynikov, and N. Stergiou, "Objective evaluation of expert and novice performance during robotic surgical training tasks," *Surg. Endos.*, vol. 23, no. 3, p. 590, 2009.